Particle swarm optimization with sequential niche technique for dynamic finite element model updating

Faisal Shabbir
Department of Civil and Environmental Engineering
The University of Auckland
New Zealand

Piotr Omenzetter **(corresponding author)**
University of Aberdeen
School of Engineering
The LRF Centre for Safety and Reliability Engineering
King's College
Aberdeen, AB24 3UE
Scotland, UK
Tel. 44-1224-272529
E-mail: piotr.omenzetter@abdn.ac.uk

ABSTRACT

Due to uncertainties associated with material properties, structural geometry, boundary conditions and connectivity of structural parts as well as inherent simplifying assumptions in the development of finite element (FE) models, actual behavior of structures often differs from model predictions. FE model updating comprises a multitude of techniques that systematically calibrate FE models in order to match experimental results. Updating of structural models can be posed as an optimization problem where model parameters that minimize the errors between the responses of the model and actual structure are sought. However, due to limited number of experimental responses and measurement errors the optimization problem may have multiple admissible solutions in the search domain. Global optimization algorithms (GOAs) are useful and efficient tools in such situations as they try to find the globally optimal solution out of many possible local minima, but are not totally immune to missing the right minimum in complex problems such as those encountered in updating. A methodology based on particle swarm optimization (PSO), a GOA, with sequential niche technique (SNT) for FE model updating is proposed and explored in this paper. The combination of PSO and SNT enables a systematic search for multiple minima and considerably increases the confidence in finding the global minimum. The method is applied to FE model updating of a pedestrian cable-stayed bridge using modal data from full-scale dynamic testing.

Keywords: cable-stayed bridge, deceptive problem, global optimization algorithms, inverse problem, model updating, multiple minima, particle swarm optimization, sequential niche technique, structural optimization

1. INTRODUCTION

Finite element (FE) modeling is nowadays routinely used for determination of responses of full-scale structures to a variety of actions, but formation of a model which replicates the behavior of the original structure with high accuracy is not easy due to inherent simplifying assumptions in model building (Friswell and Mottershead, 1995). Full-scale dynamic testing of structures often reveals important and considerable differences between the original structure and its FE model. These differences can be attributed to modeling errors associated with simplifications of complicated structural systems, inadequate discretization and parametric errors in the estimation of materials properties, geometry, and boundary and connectivity conditions.

Dynamic FE model updating is an inverse problem in which uncertain parameters of the FE model are calibrated to minimize the errors between the predictions of the FE model and experimentally measured dynamic behavior of the actual structure. Model updating can be posed as an optimization problem in which an optimal solution is sought by perturbing the uncertain parameters of the FE model so that the model prediction errors are minimized.

The number of model responses, such as natural frequencies and mode shapes, that can be determined experimentally with adequate confidence, is always limited. This can be attributed to two main reasons, namely, difficulties in identifying higher modes because of poorer signal-to-noise ratios, and difficulties arising from coarse mode shape mapping due to limited numbers of sensors used. A relatively small number of experimental responses compared to the number of uncertain parameters in the FE model may lead to the existence of multiple local minima in the solution space for the updating problem (Jaishi and Ren, 2007). Adding to that, the assumptions made in the development of FE model and uncertainties associated with material properties, boundary conditions and geometry may result in

significant differences in the natural frequencies and mode shapes obtained from the initial FE model and their experimental counterparts (Mottershead and Friswell, 1993). The algorithm searching for the global minimum of the error or objective function may then be lured into those local minima in problems that Goldberg et al. (1992) call 'deceptive'. This undesirable behavior is well known in the context of model updating. For example, the widely used sensitivity method (SM), which is essentially an iterative steepest-gradient approach sometimes combined with regularization (Titurus and Friswell, 2008), has a tendency to converge to a local minimum (Deb, 1998). Accordingly, many previous model updating studies report a single solution (Brownjohn et al., 2001; Jaishi and Ren, 2005; Zivanovic et al., 2007) but acknowledge there might be other solutions as well. A popular countermeasure is to run the updating algorithm for several times and with perturbed initial parameter values, however, such an approach is not a systematic search over the solution domain. Only limited studies have reported multiple model updating solutions and consequently the problem and its remedies have not been sufficiently explored (Zárate and Caicedo, 2008).

Global optimization algorithms (GOAs) are numerical techniques that explore the search space systematically and widely in an attempt to increase the chance of discovering the global minimum (Pintér, 1996; Price et al., 2005; Storn and Price, 1997). While there has been some documented history of their applications to model updating (Levin and Lieven, 1998; Perera and Ruiz, 2008; Tu and Lu, 2008), such studies still remain relatively limited and application of GOAs for detection of multiple minima is an active area of research in model updating problems. Coupled local minimizer (CLM) method, applicable to global optimization of a function, was proposed by Teughals et al. (2003). A population of local minimizers set up a cooperative search mechanism and was linked using synchronization constraints. CLM was successfully applied to an FE model updating problem for damage

detection in a reinforced concrete beam. Two different minima existed for the damage detection problem and CLM was able to successfully detect both of them. Bakir et al. (2008) also proposed an improved CLM technique to correctly identify damage in a complex structure. The improved CLM method was compared with Levenberg–Marquardt algorithm, sequential quadratic programming and Gauss–Newton methods and it was found that it gave better results. In another study by Zarate and Caicedo (2008), multiple admissible solutions to model updating problem were identified using the modeling-to-generate-alternatives technique. A full scale Bill Emerson Memorial bridge was updated and different plausible solutions were detected. The authors selected a solution which had a better physical justification despite having a higher error function value than the global minimum. A novel evolutionary algorithm which is able to identify local and global optimal solutions was also proposed by Caicedo and Yun (2011). This was accomplished by introducing two new operators in a genetic algorithm. The algorithm was used on a simulated numerical example of the American Society of Civil Engineers Structural Health Monitoring Benchmark structure. A random white noise was added to the acceleration records which resulted in the creation of two minima. It was found that the correct minimum had a higher objective function value than the wrong minimum. The two minima were correctly detected by the proposed algorithm. However, in these papers only a few parameters were updated in order to reduce the dimensionality of the problem and complete exploration of the search domain could not be assured. With the increase in the number of updating parameters, the behavior of the objective function becomes more complex and difficult to predict. A possible approach to such problems, which is investigated in this paper, is to perform sequential search which excludes already explored parts of the optimization domain.

One of the efficient GAOs, which is used in this study, is particle swarm optimization (PSO) (Konstantinos and Vrahatis, 2010). PSO is based on a biologically inspired

mathematical metaphor of how a swarm of bees, school of fish or similar animal grouping collectively move in search of the most fertile feeding location. Applications of PSO to model updating have so far been very limited. The algorithm performed well for model updating of simple, numerically simulated structures. Saada et al. (2008) used PSO for model updating of a beam structure, whereas a hybrid PSO-Simplex method was proposed for model updating of a ten-bar truss and a free-free beam (Begambre and Laier, 2009). Marwala (2010) applied several different GOAs to updating of the models of a simple beam and an unsymmetrical H-shaped structure and found that PSO gave better results compared to the other GOAs considered. PSO was also applied in a multi-objective optimization context to damage estimation problems with modeling errors (Perera et al., 2010). Although PSO was shown to be an efficient method for the damage estimation problem, its fast convergence sometimes led to being trapped in a local minimum.

Most recent studies which use GOAs for updating are for damage detection in laboratory structures (Perera and Torres, 2006; Perera et al., 2009b) and their suitability for model updating of full-scale structures has been inadequately explored. For example, several studies (Perera et al., 2009a; Perera et al., 2010; Raich and Liszkai, 2007) are related to the damage detection problems where the 'correct answer' (in the form of damage location) is normally known a priori to the analyst for verification of the updated results. In the context of dynamic model updating of actual, full-scale undamaged structures, the 'correct answer' is typically not known to the analyst which leads to considerable challenge in interpreting the obtained results. While, as explained earlier, GAOs in their basic form attempt to locate the global solution to an optimization problem, they cannot fully guarantee a search will always be successful. These shortcomings of GOAs in general and their previous applications to model updating motivated the approach proposed and explored in this study which is based on a systematic search over the solution domain for multiple minima of the objective function

so that the global minimum can be discovered with increased confidence. The sequential niche technique (SNT) (Beasley et al., 1993) is combined with PSO to that end. PSO is chosen due to its faster convergence speeds relative to other GOAs. SNT is simple and does not require modifications in the search algorithm itself. It only modifies the objective function after any local (or global) solution has been reached is such a way that subsequent searches avoid the vicinity of the previously found minima and are forced to search for new, yet undiscovered, ones.

The outline of the paper is as follows. In the first section, the theory of PSO and SNT are explained. Then forced vibration testing of a full-scale, cable-stayed pedestrian bridge and modal system identification are described. Next, a detailed study of updating of an FE model of the bridge is presented. Firstly, the development of an initial FE model is explained and sensitivity and uncertainty study carried out to determine the most suitable parameters for updating. PSO alone and then PSO with SNT are applied to the FE model updating problem to compare their performance. The main contributions of this study comprise a novel approach to model updating that combines PSO and SNT, and a systematic, detailed exploration of the new method performance using data from a full-scale structure.

2. THEORY

For complex optimizations problems, GOAs try to find the global minimum among many possible local minima in the search space. In model updating, the topology of the search space can be complex due to the large number of updating parameters and their influence on the objective function via numerically evaluated responses. A methodology based on combining the stochastic search algorithm PSO with SNT is proposed and investigated in this paper to improve the performance of GOA-based model updating in finding the global minimum. In the subsequent sections, the theory of PSO and SNT are explained.

2.1. Particle swarm optimization

PSO (Kennedy and Eberhart, 1995) is a population-based stochastic optimization method that iteratively tries to improve the solution with respect to a given measure of quality. The concept of PSO was developed based on the swarm behavior of fish, bees and other animals. In PSO, the members or particles making up the swarm and representing optimization parameters move in the search space in pursuit of the most fertile feeding location, or, in mathematical terms, the optimal location that minimizes an objective function. Each particle in the swarm is influenced by the rest of the swarm but is also able to independently explore its own vicinity to increase diversity. Likewise, if a swarm member sees a desirable path for the most fertile feeding location, the rest of the swarm will modify their search directions. Thus, the movement of each particle is influenced by both group knowledge and individual knowledge. It is assumed and expected that this will eventually, over a number of generations, move the whole swarm to the global optimal solution. The implementation of PSO compared to the other optimization techniques is relatively fast and cheap as there are few parameters to adjust and it can be used for a wide range of applications (Knowles et al., 2008).

In the PSO algorithm, each particle is assigned a position and velocity vector in a multidimensional space, where each position coordinate represents a parameter value. The algorithm calculates the fitness of each particle according to the specified objective function. The particles have two reasoning capabilities: the memory of their own best positions in the past generations referred to as $\mathbf{pbest}_i(t)$, and knowledge of the overall swarm best position referred to as $\mathbf{gbest}(t)$. The position $\mathbf{x}_i(t)$ of each particle is updated in each generation by the simple recursive formula (see also Figure 1):

$$\mathbf{x}_i(t+1) = \mathbf{x}_i(t) + \mathbf{v}_i(t+1) \tag{1}$$

where i is the particle number and t is the generation number. The velocity of each particle $\mathbf{v}_\mathrm{i}(t)$ towards its **pbest**$_i(t)$ and **gbest**(t) locations is adjusted in each generation using the following formula:

$$\mathbf{v}_\mathrm{i}(t+1) = \gamma \times \mathbf{v}_\mathrm{i}(t) + c_1 \times rand_1 \times \left(\mathbf{pbest}_\mathrm{i}(t) - \mathbf{x}_\mathrm{i}(t)\right) + c_2 \times rand_2 \times \left(\mathbf{gbest}(t) - \mathbf{x}_i(\mathrm{t})\right) \tag{2}$$

where $\mathbf{v}_i(t)$ is the initial velocity, $\mathbf{v}_i(t+1)$ is the updated velocity, γ is the inertial weight, c_1 and c_2 are the cognition and social coefficient, and $rand_1$ and $rand_2$ are random numbers uniformly distributed between 0 and 1, respectively.

In addition to the inertia term that holds the memory of all previous iterations, there are two terms in Equation (2): one related to the particle's local best position which defines the exploitative behavior, and the other related to the best global position which defines the swarm exploratory behavior (Konstantinos and Vrahatis, 2010). The exploitative behavior is related to local search where a given particle tries to get closer and closer to the (possibly local) minimum, whereas the exploratory behavior is related to the search of a broader region of the parameter domain by the entire swarm. To avoid premature convergence, the cognition and social component coefficient, c_1 and c_2, should be carefully selected. A constraint on the maximum velocity of the particle can also be imposed to ensure that the particles remain within the maximum and minimum bounds. Both theoretical and empirical studies have been undertaken to help in selecting the values of these parameters (Pedersen and Chipperfield, 2010; Trelea, 2003; Zheng et al., 2003).

2.2. Sequential niche technique

The principle of SNT is to carry over knowledge gained during subsequent iterations of an optimization algorithm (Beasley et al., 1993) so that different minima are discovered one by one. The basic idea behind SNT is that when a minimum is found in the search domain, the surrounding area, referred to as niche, is 'filled in' and no longer attracts the particles in subsequent iterations. This forces the optimization algorithm to converge to another, yet unvisited, niche. The process continues until the criteria such as the maximum number of iterations, maximum number of discovered minima and the upper threshold value of the objective function at a minimum have been met.

Initial iterations in search of the first minimum are made with the basic search algorithm, PSO in this case, without SNT by using the raw objective function. Once the first minimum has been found, the objective function values of the particles in the vicinity of the minimum are modified, and the search for the next minimum commences. The modifications to the objective function are introduced by multiplying it by a derating function using the following recursive formula:

$$\prod_{n+1}(\mathbf{x}) = \prod_{n}(\mathbf{x}) \times G(\mathbf{x}, \mathbf{s}_n) \tag{3}$$

where $\prod_{n+1}(\mathbf{x})$ is the modified objective function to be used for searching for the n+1-th minimum, $\prod_{n}(\mathbf{x})$ is the previous objective function used for searching for the n-th minimum, $G(\mathbf{x}, \mathbf{s}_n)$ is the derating function, and $\mathbf{s}_n$ is the n-th found minimum.

The following exponential derating function is used in this study (Beasley et al., 1993):

$$G(\mathbf{x}, \mathbf{s}_n) = \begin{cases} exp\left(log\ m \times \dfrac{r - d(\mathbf{x}, \mathbf{s}_n)}{r}\right) & if\ d(\mathbf{x}, \mathbf{s}_n) < r \\ 1 & otherwise \end{cases} \tag{4}$$

where m is the derating value used to control concavity of the derating function, r is the niche radius, and $d(\mathbf{x}, \mathbf{s}_n)$ defines the distance between the current point $\mathbf{x}$ and the previously found minimum $\mathbf{s}_n$.

The niche radius r is an important parameter as it is used to define the size of the part of the search domain in the neighborhood of a minimum where the objective function is modified. Smaller values of niche radii produce more concavity in the derating function and limit the spatial extent of its effect but may introduce low value spurious minima, while larger niche radii can affect the other true minima in the search space. The niche radius has been determined in this study by the method proposed by Deb (1989) who suggested using a value calculated as

$$r = \frac{\sqrt{k}}{2 \times \sqrt[k]{p}} \tag{5}$$

where k represents the dimension of the problem (the number of parameters) and p is the expected number of minima. Each parameter has to be normalized between 0 and 1 for the use of SNT. This approach assumes that all minima are fairly equally distributed throughout the search domain. However, since the distribution of minima was not known a priori, a value equal to 50% of that calculated from Equation (5) was used.

3. BRIDGE DESCRIPTION

The full-scale structure under study is a 59,500 mm long cable-stayed footbridge with two symmetrical spans supported on abutments, a central A-shaped pylon and six pairs of stays as shown in Figure 2. Figure 3 shows the deck cross-section, which comprises a trapezoidal steel girder with overhangs of a total width of 2,500 mm and depth of 470 mm, made of 16 mm thick plates, and a non-composite concrete slab of thickness 130 mm. The concrete

slab was assumed in design to provide no contribution to the deck stiffness, although its mass and weight were accounted for. Closed steel rectangular pipes having a cross-section of 250× 150×9 mm also run on both sides of the bridge deck and enclose two 100 mm ducts for service pipes with surrounding void spaces filled with grout. Railing was provided on both sides of the bridge and it has a total height of 1,400 mm. The sections of railings were disconnected from each other at every 8,000 mm.

The girder is continuous over the entire bridge length. It is supported on two elastomeric pad-type bearings of dimensions 90×180×12 mm at the central pylon. At each abutment two 150×150×12 mm elastomeric pad-type bearings are also provided, but these have a special arrangement that allows for longitudinal sliding while constraining any lateral horizontal displacements. The sliding bearings were provided to accommodate creep, shrinkage and temperature deformations, and to allow the bridge to move longitudinally in the event of a strong seismic excitation. The distance between bearing axes is 450 mm. The abutments are supported by two concrete piles, and 10 concrete piles and a pile cap are used at the central pylon.

The six pairs of stay cables are fixed to the deck at distances of about 8,000 mm center to center as shown in Figure 4. All the cables have a diameter of 32 mm. Different post-tension forces, ranging from 55 kN to 95 kN in each cable, were specified in design. The cables were connected to the top of the 22,400 mm high center pylon, which is composed of two steel I-sections joined with cross bracing that supports the deck. The size of the pylon I-sections is 400WC328 (AS/NZS, 1996).

4. EXPERIMENTAL PROGRAM AND SYSTEM IDENTIFICATION

Experimental work has been carried out using uni-axial Honeywell QA 750 accelerometers to measure structural response, uni-axial Crossbow CXL series MEMS accelerometers to measure shaker input force and a desktop computer fitted with an NI DAQ 9203 data acquisition card. Data was collected at a sampling rate of 200 Hz. Three APS ElectroSeis Model 400 shakers (APSDynamics, 2012), capable of providing a combined dynamic force of up to 1.2 kN, were used in a synchronized mode to impart excitation to the structure.

Full scale tests can be conducted by output only (no measured force) or input-output (measured force) methods. The cable stayed bridge under study has been tested using both of these methods. The output only test was conducted using jumping to establish the initial estimation of the natural frequencies of the bridge. Two people jumped on the bridge in unison to excite the structure and thereafter the bridge was allowed to freely vibrate for two minutes. This was done to establish the range of excitation frequencies for subsequent forced vibration tests. Following that, a sweep sine excitation ranging from 1 Hz to 15 Hz with a total duration of 391 seconds was adopted to excite the structure. The shakers were located away from the center line of the deck to excite both the vertical and torsional modes. To excite horizontal modes, the shakers were tilted at 90º. Figure 4 shows the locations of the shakers and accelerometers on the bridge during testing. Accelerometers were placed on both sides of the deck to capture vertical and torsional responses. Figure 5 shows the QA 750 accelerometers and shakers placed on the bridge deck for horizontal forcing. One of the accelerometers was also placed on the bridge abutment to measure its response. Figure 6 shows the time history of force delivered by a shaker, and Figure 7 shows the time history of bridge response recorded by one of the accelerometers during vertical testing. It can be seen in Figure 7 how subsequent modes are excited as the shakers sweep through the

corresponding modal resonant frequencies. The vertical and horizontal tests were repeated twice to ensure good quality data.

For system identification in the frequency domain, peak picking using frequency response function (FRF) is a simple and commonly used method (Ewins, 2000). FRF is a measure of system response to the input signal at each frequency and can be calculated from the auto-spectrum of excitation and cross-spectrum between response and excitation (Friswell and Mottershead, 1995). For calculating the spectra, the Welch averaging method was used (Proakis and Manolakis, 1996) with each time history divided into five segments with 50% overlap and Hamming windowing. Finally, FRFs from the available experiments were averaged. To assess the quality of a FRF and distinguish between real and spurious peaks coherence can be used (Ewins, 2000). Coherence can be calculated using the aforementioned spectra and the auto-spectrum of response. High coherence values, close to one, indicate that response at a given frequency is caused by the measured input rather than other sources of excitation or is a false result introduced by noise. An example of a FRF obtained during a vertical shaker test is shown in Figure 8, where FRF modulus or magnitude, phase and coherence are shown. It can be noticed that the magnitude has peaks at 1.64 Hz, 1.90 Hz, 3.66 Hz, 6.32 Hz, 7.42 Hz and 8.33 Hz. All but the last peak at 8.33 Hz, which is a torsional mode, correspond to vertical modes. Higher peaks are observed at modes corresponding to 6.32 Hz and 7.42 Hz, which shows that these modes are responding more strongly than the others. Also, the torsional mode peak at 8.33 Hz is less clearly visible possibly due to low levels of excitation torque delivered by the shakers. The phase of the FRF shows a change by 180° close to 1.64 Hz, 1.90 Hz, 3.66 Hz, 6.32 Hz, 7.42 Hz and 8.33 Hz further confirming these are modal frequencies. The phase change is again much clearer at 6.32 Hz and 7.42 Hz as they are better excited than the other modes. The coherence between excitation and response have values of more than 0.8 at 1.64 Hz, 1.90Hz, 3.66 Hz, 6.32 Hz, 7.42 Hz and

8.33 Hz, indicating that a reasonably good correlation exists between the force and response signals. Much better coherence values, very close to one, were observed at 6.32 Hz and 7.42 Hz. Some other peaks, e.g. just above 10 Hz, can also be seen but the corresponding coherence values are low. Similarly, two resonance frequencies were identified using horizontal shaker excitation at 4.85 Hz and 5.36 Hz, respectively.

The well-known challenges of in-situ testing of full-scale large systems, like bridges, must be kept in mind while assessing the quality of the obtained FRFs. These include, but are not limited to, poorer signal-to-noise ratios because of limited capacity of exciters, very limited control of several ambient sources of excitation and noise (wind, construction works, vehicles, occupants, machinery, etc. – some of which are always present), and limited data as, unlike in the lab, tests cannot typically be repeated tens or hundreds of times for averaging. Given those challenges, it can be concluded that experimental data of sufficient quality have successfully been acquired.

For cross-checking the results of pick peaking and also to identify damping ratios and mode shapes the numerical algorithm for subspace state-space system identification (N4SID) technique (Van Overschee and De Moor, 1994), operating in time domain and utilizing a subspace identification algorithm, was used. The general subspace algorithm (Overschee and Moor, 1996) can be applied to both input-only and input-output identification. In these approaches, state space system matrices are first obtained from the measurements, and then natural frequencies, damping ratios, and mode shapes can then be derived from these system matrices.

The adequate order of the state space model needs to be carefully determined. Theoretically, the system order should be twice the number of the degrees of freedom, i.e. modes, of interest. However, due to measurement noise a higher model order is normally

required to extract the modes of interest with higher confidence and discard spurious, artificial results. To that end, stability diagrams are employed. As the system order increases, the structural modes identified by the algorithm should remain consistent and stable (Bodeux and Golinval, 2001). The model orders selected for this study ranged from 10 to 80 for the vertical shaker configuration. Stability thresholds were selected based on previous experience and data quality. A threshold of 1% for frequency variation and a value above 0.8 for modal assurance criterion (MAC) (Allemang and Brown, 1982) between two subsequent model orders were used. MAC for two mode shapes, $\emptyset_i$ and $\emptyset_j$, is defined as

$$MAC = \frac{|\emptyset'_i \emptyset_j|^2}{(\emptyset'_i \emptyset_i)(\emptyset'_j \emptyset_j)} \quad (6)$$

where the apostrophe denotes vector transposition. MAC takes a value of one for perfectly correlated modes and zero for two orthogonal modes.

The stability diagram for a vertical shaking test is shown in Figure 9. It can be seen from the stability diagram that the six previously observed modes, five vertical and one torsional, are stable and can be identified from the vertical tests as shown by the black dots in the figure. Some spurious modes, that did not meet the stipulated stability criteria, were also detected as shown by the white dots in the figure. In a similar way, two modes previously seen in the FRFs were identified from the horizontal tests.

Table 1 summarizes the natural frequencies identified from the peak picking and N4SID method. It can be seen from the results that the frequencies identified by both methods match very well. The damping ratios identified by the N4SID method are also shown in Table 1. It is observed that damping in the bridge is small, ranging between 0.2% and 1.4%.

Five vertical, two horizontal and one torsional mode shape identified from modal tests using the N4SID method are shown in Figure 10. It has been observed from the system identification results that the first two vertical modes have nearly identical sinusoidal shapes over the length of the bridge. An additional accelerometer was attached to one of the cables closest to the abutments during the vertical shaker tests and it has been found that the cable vibrates laterally at the frequency of the second mode, i.e. at 1.89 Hz. Thus, the pattern of cable vibration differentiates these two modes.

Only one torsional mode of the system was identified by the forced vibration tests at 8.32 Hz. Typically, one would expect a torsional mode of a shape similar to a full sinusoid where the deck twists in the opposite directions in each span (Ren and Peng, 2005). However, in the observed torsional mode the whole deck twists in the same direction. The reason behind this is that the main girder is a closed trapezoidal cross-section (Figure 3) thus having a large torsional stiffness, which makes it difficult to twist the bridge deck in a full-sine pattern. Also, the closed rectangular pipes with service ducts and railing that run near the edges throughout the length of the bridge further increase the torsional stiffness of the deck. It is thus easier to deform the pylon resulting in the torsional mode shape as indicated in Figure 10.

5. BRIDGE FINITE ELEMENT MODEL

There are many ways to model cable-stayed bridges to obtain a realistic representation of their dynamic behavior. The main elements to be modeled are the deck, pylon, cables, and connections of cables and deck. A good representation of bridge deck for box girder sections can be achieved by using beam elements with rigid links joining the cable elements with the deck elements (Chang et al., 2001; Ren and Peng, 2005). In this research, the bridge was modeled in SAP2000 (2009) and the FE model is shown in Figure 11. The deck and pylon

were modeled using beam type FEs. The deck was discretized into 48 elements, whereas the pylon was discretized into 40 elements. These numbers of elements were selected as further discretization did not appreciably affect the results of numerical modal analysis of the first eight modes and only resulted in an increased computational cost. The cables were modeled using catenary elements provided in SAP2000 and were discretized into four elements for each cable. As indicated earlier, the first two experimentally identified vertical modes (Figure 10) have very similar shapes of girder vibrations and an initial FE model with no discretization of the cables did not show the second of the two modes. After discretization of the cables into four elements all the experimentally observed modes were correctly replicated by the FE model.

The modulus of elasticity for steel was taken as 200 GPa, for cables as 165 GPa and for concrete as 28 GPa following available design specifications. The cast is situ concrete slab was assumed to be fully composite with the steel girder resulting in a combined cross-sectional second moment of inertia of 0.06140 m^4 for horizontal bending, 0.00439 m^4 for vertical bending and torsional constant of 0.00810 m^4. (Note that this contradicts the assumption made in design that there is no contribution from the slab to the stiffness of the deck. However, it was anticipated that partial composite action between the steel and concrete did exist, as is often the case in real structures, and its actual extent will be quantified via model updating later.) An initial non-linear static analysis was performed to account for the geometric non-linearity caused by the cable sag and this was followed by a linear dynamic analysis to obtain natural frequencies and mode shapes. A linear analysis that uses stiffness from the end of non-linear static analysis for cable-stayed structures has been demonstrated to provide good results in previous studies (Abdel-Ghaffar and Khalifa, 1991).

The response of the bridge was also measured with sensors on the bridge abutment beneath the deck. The abutment did not show any appreciable response in the vertical or

horizontal direction and so both abutments were ignored in the FE model. However, the stiffness of the bearings for shear and compression have been considered in the model and calculated using the procedure proposed by Gent (2012). The formulas take into account the effective load area, thickness of bearing and its shape, and Young's and shear moduli of the elastomer. Furthermore, as explained before the distance between bearing axes is 450 mm and the torsional restraint provided by the bearings was also taken into account (Jaishi and Ren, 2007). The Young's and shear moduli were assumed after Gent (2012) as 3.2 GPa and 0.8 GPa, respectively. The shear, vertical and torsional stiffness for springs modeling the pylon bearing were found to be 2.14×10^6 N/m, 7.70×10^7 N/m and 3.90×10^6 Nm/rad, respectively. The stiffness for vertical and torsional springs modeling the abutment bearings were found to be 1.60×10^8 N/m and 8.86×10^8 Nm/rad, respectively. No shear deformations were allowed at the abutment. The freedom of the abutment bearings to slide in the longitudinal direction was ignored; this was not expected to have any strong effects on the model accuracy as neither was the bridge excited in the longitudinal direction during dynamic tests, nor were the corresponding modes identified or considered in the analysis. Lateral horizontal displacements at the abutments were constrained as previously explained.

Table 2 summarizes the errors between experimental frequencies and mode shapes and those identified by the initial FE model. To compare experimental and numerical mode shapes MAC (Equation (6)) was used. It has been found that the frequencies obtained from the initial FE model differ from the experimental frequencies by up to 8.64% and MAC values are between 0.980 and 0.999. The systematic attempts to improve the agreement between the experimental and numerical predictions via PSO and SNT-based model updating are discussed in the next section.

6. BRIDGE MODEL UPDATING

In model updating, dynamic measurements such as natural frequencies and mode shapes are correlated with their FE model counterparts to calibrate the FE model. There is a degree of uncertainty in the assessment of the actual properties of the materials used in the full-scale structure as well as the most realistic representation of the element stiffness, supports and connections between structural parts in the initial FE model. The challenge of finding a set of suitable parameters having physical justification necessitates the need for use of physically significant updating parameters and suitable optimization tools.

6.1. Objective function for model updating

An objective function quantifies the deviation of the analytical predictions of modal parameters from those obtained experimentally. The following objective function is used in this study:

$$\Pi = \alpha_1 \sum_{i=1}^{n} \left(\frac{f_{a,i} - f_{e,i}}{f_{e,i}} \right)^2 + \alpha_2 \sum_{i=1}^{m} \frac{(1-\sqrt{MAC_i})^2}{MAC_i} + \alpha_3 \Pi_r \quad (7)$$

The first term is the total relative difference between the experimental and analytical frequencies, where f represents the frequency, subscripts a and e refer to analytical and experimental, respectively, and n is the total number of frequencies considered. The second term measures the difference in mode shapes in terms of MACs (Möller and Friberg, 1998), where m is the total number of modes considered. The third term, Π_r is related to regularization and for time being it is given in a general form to be specified later, once the sensitivity of frequencies to the proposed updating parameters is examined. Regularization in model updating is often introduced for ill posted problems that may not have a unique solution (Ahmadian et al., 1998; Friswell and Mottershead, 1995; Hua et al., 2009; Mottershead and Foster, 1991; Titurus and Friswell, 2008). Regularization, following the

original idea by Tikhonov (1963), augments the objective function with new conditions, that dependent on updating parameters rather than the measured responses, in order to steer optimisation into the regions of search space where it is assumed or believed their values belong. Finally, α_1 through α_3 are weighting factors allowing for relative promotion and demotion of the error terms.

6.2. Selection of updating parameters

The selection of parameters in model updating is critical for the success of any such exercise. An excessive number of parameters compared to the number of available responses, or overparametrization, will lead to a non-unique solution, whereas insufficient number of parameters will prevent reaching a good agreement between the experiment and numerical model (Titurus and Friswell, 2008). Updating parameters are selected with the aim of correcting the uncertainties in the FE model. It is necessary, therefore, to select those parameters to which the numerical responses are sensitive and whose values are uncertain in the initial model. Otherwise, the parameters may deviate far from the initial FE model and take on meaningless values while still resulting in good correlations between numerical and experimental results.

The discrepancies between the different parameters of the initial FE model and the full-scale structure can be attributed to many inherent uncertainties and modeling assumptions, such as material density, stiffness and boundary and connectivity conditions. Parameter selection therefore requires a considerable insight into the structure and its model. In this study, only a relatively small number of parameters were selected based on a prior knowledge of their potential variability, and a sensitivity analysis was carried out to confirm they influence the responses. The various inertia parameters of the structure were not included as these are typically less uncertain than stiffness parameters. The bridge was also

supported at clearly defined points using specialized bearings that permitted making good judgment about the appropriate modeling of boundary conditions, except the numerical values of bearing spring stiffness. Thus, candidate parameters considered for calibration in this study were cable tensions, cable axial stiffness, bending and torsional stiffness of the deck and stiffness of the bearings.

The likely uncertainty of the parameters characterizing cable stiffness, i.e. cable axial stiffness and tension force, can be attributed to many factors such as application of different tensioning forces than those specified in design, relaxation of steel stresses with time, and slippage in anchorages and between cable strands. Stiffness of the deck depends on Young's modulus of both steel and concrete; especially the latter shows considerable variability. The connection between steel girder and concrete slab will typically be designed to allow for either composite action or lack thereof. However, real bridges will always exhibit a certain degree of composite action (less than full because of connector flexibility, and more than none because of, for example, steel-concrete bond and friction) eluding the analyst. Furthermore, non-structural elements, such as pavement, railings, services, also make a contribution to stiffness that is difficult to quantify and model precisely. Also, stiffness of the bearings was assumed from literature as the exact specifications were not known, and is thus prone to uncertainty further exacerbated by the inherent variability of elastomer properties.

There are three pairs of stay cables on each side of the central pylon. The four identical cables closest to the abutments are referred to as Cab-1, the four cables in the middle as Cab-2, and the four cables nearest to the pylon as Cab-3 (Figure 4). The cables were post-tensioned, as per design documentation, with forces $T_{Cab\text{-}1}$=55kN for the four cables closest to the abutments, $T_{Cab\text{-}2}$=95kN for the middle cables, and $T_{Cab\text{-}3}$=75kN for the cables nearest to the central pylon (Figure 4). The effective axial stiffness of a cable depends on its projected length, self-weight, axial stiffness EA (where E is Young's modulus and A is

cross-sectional area) and tension force in the cable (Nazmy and Abdel-Ghaffar, 1990). For taut cables with small sag, the influence of axial stiffness *EA* on the effective stiffness is more pronounced than that of the tension force. A simple hand calculations using the Ernst formula for cable stiffness (Nazmy and Abdel-Ghaffar, 1990) showed that the effect of tension force on stiffness is much more important in cables Cab-1 compared to the remaining cables. This was later confirmed by the sensitivity analysis on the FE model, and therefore only tension $T_{Cab\text{-}1}$ was included in the updating parameters.

Sensitivity analysis using the FEM model was conducted to confirm the selected updating parameters can influence the analytical responses. Relative sensitivity is the ratio of the relative change in the response value caused by a relative change in the parameter value. In this study, sensitivities were calculated using a finite difference method by changing the parameters by 0.1% with respect to their initial values. The selected parameters based on sensitivity analysis and engineering insight into their uncertainty were deck flexural stiffness for vertical ($K_{y,deck}$) and horizontal ($K_{x,deck}$) bending, deck torsional stiffness ($K_{t,deck}$), axial stiffness of all cables (K_{cable}), cable tension for Cab-1 ($T_{Cab\text{-}1}$), and stiffness of bearings ($K_{bearing}$). The bearing stiffness, $K_{bearing}$, is to be understood as a single parameter whose changes affect proportionally the stiffness of bearing springs in the horizontal, vertical and torsional direction; this was done to keep the number of bearing related updating parameters to a minimum.

The sensitivities of modal frequencies to the updating parameters are shown in Figure 12. It can be noticed from the figure that, as can be expected, parameters $K_{y,deck}$, K_{cable} and $T_{Cab\text{-}1}$ influence appreciably, albeit to a varying degrees, the frequencies of vertical Modes 1, 2, 3, 6 and 7. Additionally, K_{cable} influences the torsional Mode 8. Parameter $K_{x,deck}$ influences the horizontal Modes 4 and 5. Two of the parameters that influence the torsional Mode 8, $K_{bearing}$ and $K_{t,deck}$ require careful attention. Ignoring a very small influence $K_{bearing}$ has on

other modes, the two parameters practically only influence Mode 8. It can thus be expected, and indeed it was confirmed in preliminary calculations, that without constraining the two parameter variations attempts to update Mode 8 will create an ill posed problem with no unique solution. To overcome the problem, a regularization constraint was applied to keep the ratio of $K_{t,deck}/K_{bearing}$ approximately constant during updating. The objective function, given in its general form in Equation (7), now becomes as follows:

$$\Pi = \sum_{i=1}^{n}\left(\frac{f_{a,i}-f_{e,i}}{f_{e,i}}\right)^2 + \sum_{i=1}^{m}\frac{(1-\sqrt{MAC_i})^2}{MAC_i} + 0.0002 \times \left|\frac{K_{t,deck,j}}{K_{bearing,j}} - \frac{K_{t,deck,0}}{K_{bearing,0}}\right| \quad (8)$$

where subscript j in the regularization part denotes current values of parameters and subscript 0 represents their initial values. The value of the regularization term weighting factor α_3=0.0002 (Equation (6)) was adjusted by trial and error so that the ratio of the two parameters did not change more than ±10%. It is acknowledged here that the way the two parameters were linked can be considered arbitrary, but it can also be argued to be physically plausible. Furthermore, the examination of the potential ill posing of the problem by checking the sensitivity plot should in future be performed in a more systematic and rigorous way.

Finally, selecting appropriate bounds on the allowable parameter variations during model updating is challenging and is normally done using engineering judgment. Different bounds have been used in previous research (Jaishi and Ren, 2005; Zivanovic et al., 2007). From the frequency errors in Table 2, it can be concluded that the initial FE model generally overestimates the stiffness, therefore the lower bound has been selected as -40% and the upper bound was selected as +30% for all the parameters.

6.3. Assessment of the performance of model updating methodology

This section applies the proposed method to updating of the pedestrian bridge FE model in order to explore the performance of the approach. All the eight experimentally identified

modal frequencies and mode shapes were used. A population of 30 particles was used by the PSO algorithm, the maximum number of generations was set to 200, and the upper threshold of the objective function to 0.001. The selection of parameters in the PSO algorithm is critical to its success. On the basis of extensive studies conducted by Clerc and Kennedy (2002), the PSO parameters appearing in Equation (2) were set to γ =0.729, c_1=1.5 and c_2= 1.5 (known as the default contemporary PSO variant). The maximum velocity has been constrained as half of the allowable parameter variation range (-40% - +30%). The niche radius for SNT was calculated according to Equation (5) for four minima as 0.97, but to account for possible closeness of some of these minima 50% of this value was adopted. The parameter *m* for derating function (Equation (4)) was assumed as 1000.

Model updating by PSO alone, i.e. without SNT, was attempted first. Ten independent runs were tested with different, randomly selected starting points. The purpose of these simulations was to see if PSO would be drawn to local minima. The best solution (i.e. the one giving the smallest value of the objective function) from the 10 runs is shown in Table 3 in the form of the ratios of updated to initial stiffness values. Standard deviations of these stiffness ratios from the 10 runs are also listed in Table 3 in parentheses to help in judging how many minima were encountered by PSO alone. It can be seen that the maximum standard deviation of the updated parameter ratios is only 0.0058, giving confidence that all the solutions correspond to the same point in the search space.

Although PSO alone convincingly converged to the same minimum during all trials with random starting points, it is worthwhile to explore systematically the search space for multiple minima and to that end PSO with SNT was applied. PSO with SNT was iterated five times with random starting points and the results are shown in Table 4. Again, the best solution reached for each minimum is reported but standard deviations for five runs were of a similar small order as in the case of PSO alone. It can be seen that the first minimum found is

the same minimum as the one found earlier by PSO alone. In further iterations, different minima with increased objective function values were found. Also, the updated parameter values for those minima were in many cases quite different than for the first minimum. This is because SNT forbids the search algorithm to converge again to the same niche. The systematic search using PSO with SNT gave an increased confidence in finding the global minimum.

For checking the effect of the niche radius, the raw objective function values were compared with the modified function values obtained after the derating function was applied. It has been found that the niche radius used in this study has not affected the other minima in the search space.

The initial and updated frequencies, their errors compared to the experimental results, and MACs between the updated and experimental mode shapes are shown in Table 5. All frequency errors are generally less than 3% after updating. The largest error dropped from 8.64% to 2.84%, and in fact corresponds to a small error increase for the first vertical mode. This indicates that it is possible to improve the FE model considerably via adjusting the particular set of updating parameters considered, but some trade-off are inevitable. On the other hand, MAC values did not change appreciably, with some small positive and negative changes in different mode and the minimum value is 0.987. MAC values, however, were already very good in the initial FEM model.

The updated parameters should be physically meaningful; otherwise it is difficult to justify the updating results. The vertical bending stiffness of the bridge deck has decreased to 84.5%, horizontal stiffness to 83.7% and torsional stiffness to 93.5%, respectively. This could be mainly attributed to the fact that the initial model takes the cast in-situ concrete slab as fully composite with the steel girder, whereas no concrete contribution to deck stiffness was

assumed in design and, consequently, no special shear connectors were provided. (For comparison, when one ignores the concrete slab, the deck stiffness is 84.6%, 73.6% and 60.9% for vertical bending, horizontal bending and torsional stiffness, respectively, compared to the fully composite case.) The updated results reveal that there may be some, albeit at best only partial, composite action between the slab and the steel girder contributing to the stiffness of the whole deck. The consistent decrease in all the parameters related to the deck stiffness supports this conclusion. Nevertheless, different than assumed stiffness of concrete and steel girder (e.g. due to stiffeners), and non-structural components can also be responsible. However, with only the limited number of measured modes available, further granularity in girder stiffness modeling cannot be further conclusively explored and has to be acknowledged as a limitation of this updating exercise.

The bearing stiffness has decreased to 93.2%, which is a plausible reduction given that the initial value was assumed from literature. Due to the regularization term included in Equation (10), the values of the updated bearing stiffness and torsional stiffness of the deck change in a similar relative way. The increase in cable tension $T_{Cab\text{-}1}$ to 116.0%, shows that these post-tension forces are more than the designed value of 55 kN, indicating some possible overstressing of the cables. On the other hand, the cable axial stiffness shows a drop to 92.5%. The latter result can be attributed to many factors. The FEM model uses a rather coarse parameterization. As a result, potential localized stiffness changes may be lumped into those parameters. For example, the identified drop in the cable axial stiffness may well be because of slippage in the cable anchorages, i.e. uncertainty in the modeling of structural connectivity. Uncertainties in material properties and slippage between cable strands can be influencing factors too. In general, the updated model represents the optimal solution for the optimization problem of Equation (8) that is also justified by engineering judgment, but

hinges on the validity of the initial model topology, discretization and parameterization. We argue that these are adequate.

As with any multiple minimum inverse or identification problem which is, for practical reasons, solved numerically, no absolute assurance can ever be given that the chosen solution is undeniably correct, and so careful engineering judgment is required. Examining the results reported in Table 4, it can be seen that the other minima found not only are associated with higher objective function values but also results in less realistic updated mechanical parameters. For example, more significant drops of stiffness of the deck and bearings (up to 40%) can be seen accompanied by more significant (up to 30%) increases in cable–related parameters. These reasons provide sufficient ground to argue that our chosen solution is the closest to the true dynamics of the bridge.

The application of PSO combined with SNT increases the confidence in the obtained results as most of the solution space has been searched sequentially. The user, based on engineering judgment, can select the best solution from a list of different available solutions. The results demonstrate how a multi-dimensional search space can be systematically explored and how the applicability of updating techniques can be extended to more challenging problems.

7. CONCLUSIONS

A combination of PSO and SNT has been proposed in this study to systematically explore the search domain in updating problems with multiple minima. SNT works by ‘filling in’ the objective function niches, corresponding to the already known minima, and forces PSO to expend its region of search, thereby increasing the chance of finding the global minimum. The performance of PSO augmented with SNT has been explored using experimental modal analysis results from a full-scale cable-stayed pedestrian bridge. The results show that the

methodology proposed herein gives the analyst more confidence in the model updating results and that it can successfully be applied to more challenging full-scale structures. The paper also emphasized that no updating exercise can rely on numerical results alone and careful interpretation and physical justification of the results are indispensable.

ACKNOWLEDGMENTS

The authors would like to express their gratitude to organizations and people that supported this research. Faisal Shabbir would like to acknowledge Higher Education Commission of Pakistan for funding his PhD studies. Piotr Omenzetter's work within The LRF Centre for Safety and Reliability Engineering at the University of Aberdeen is supported by Lloyd's Register Foundation (LRF). LRF, a UK registered charity and sole shareholder of Lloyd's Register Group Ltd, invests in science, engineering and technology for public benefit, worldwide. Ben Ryder of Aurecon and Graeme Cummings of HEB Construction assisted in obtaining access to the bridge and information for modeling. Luke Williams and Graham Bougen, undergraduate research students, assisted with testing.

REFERENCES

Abdel-Ghaffar, A.M., & Khalifa, M.A. (1991), Importance of cable vibration in dynamics of cable-stayed bridges, *Journal of Engineering Mechanics, ASCE*, 117, 2571-2589.

Ahmadian, H., Mottershead, J.E., & Friswell, M.I. (1998), Regularization methods for finite element model updating, *Mechanical Systems and Signal Processing*, 12, 47-64.

Allemang, R.J., & Brown, D.L. (1982), A correlation for modal vector analysis, *Proceedings of IMAC I : 1st International Modal Analysis Conference*, 110-116.

APSDynamics (2012), Dynamic ElectroSeis shaker Model 400. http://www.apsdynamics.com/

AS/NZS (1996), *AS/NZS 3679 Part-1 Structural steel hot rolled bars and sections*, Jointly published by Standards Australia, Sydney and Standards New Zealand, Wellington.

Bakir, P.G., Reynders, E., & Roeck, G.D. (2008), An improved finite element model updating method by the global optimization technique 'Coupled Local Minimizers', *Computers & Structures*, 86, 1339-1352.

Beasley, D., Bull, D.R., & Martin, R.R. (1993), A sequential niche technique for multimodal function optimization, *Evolutionary Computation*, 1, 101-125.

Begambre, O., & Laier, J.E. (2009), A hybrid Particle Swarm Optimization - Simplex algorithm (PSOS) for structural damage identification, *Advances in Engineering Software*, 40, 883-891.

Bodeux, J.B., & Golinval, J.C. (2001), Application of ARMAV models to the identification and damage detection of mechanical and civil engineering structures, *Smart Materials and Structures*, 10, 479-489.

Brownjohn, J.M.W., Xia, P.Q., Hao, H., & Xia, Y. (2001), Civil structure condition assessment by FE model updating : methodology and case studies, *Finite Elements in Analysis and Design*, 37, 761-775.

Caicedo, J.M., & Yun, G. (2011), A novel evolutionary algorithm for identifying multiple alternative solutions in model updating, *Structural Health Monitoring*, 10, 491-501.

Chang, C.C., Chang, T.Y.P., & Zhang, Q.W. (2001), Ambient vibration of long-span cable-stayed bridge, *Journal of Bridge Engineering, ASCE*, 6, 46-53.

Clerc, M., & Kennedy, J. (2002), The particle swarm - explosion, stability, and convergence in a multidimensional complex space, *IEEE Transactions on Evolutionary Computation*, 6, 58-73.

Deb, K. (1989), *Genetic algorithms in multimodal function optimization*, M.S. Thesis, The University of Alabama,Tuscaloosa, AL.

Deb, K. (1998), *Optimization for engineering design : algorithms and examples*, Prentice-Hall of India, New Delhi.

Ewins, D.J. (2000), *Modal testing : theory, practice, and application*, Research Studies Press, Baldock, Hertfordshire, England.

Friswell, M.I., & Mottershead, J.E. (1995), *Finite element model updating in structural dynamics*, Kluwer Academic Publishers, Netherlands.

Gent, A.N. (2012), *Engineering with rubber - how to design rubber components (3rd Edition)*, Munich, Cincinnati, Hanser Publishers.

Goldberg, D.E., Deb, K., & Horn, J. (1992), Massive multimodality, deception, and genetic algorithms, *Parallel Problem Solving from Nature*, 2, 37-46.

Hua, X.G., Ni, Y.Q., & Ko, J.M. (2009), Adaptive regularization parameter optimization in output-error-based finite element model updating, *Mechanical Systems and Signal Processing*, 23, 563-579.

Jaishi, B., & Ren, W.X. (2005), Structural finite element model updating using ambient vibration test results, *Journal of Structural Engineering, ASCE*, 131, 617-628.

Jaishi, B., & Ren, W.X. (2007), Finite element model updating based on eigenvalue and strain energy residuals using multiobjective optimisation technique, *Mechanical Systems and Signal Processing*, 21, 2295-2317.

Kennedy, J., & Eberhart, R. (1995), Particle swarm optimization, *IEEE International Conference on Neural Networks*, 4, 1942-1948.

Knowles, J., Corne, D., & Deb, K. (2008), *Multiobjective problem solving from nature: from concepts to applications*, Springer-Verlag, New York.

Konstantinos, E.P., & Vrahatis, M.N. (2010), *Particle swarm optimization and intelligence : advances and applications*, Information Science Reference, Hershey, PA.

Levin, R.I., & Lieven, N.A.J. (1998), Dynamic finite element model updating using simulated annealing and genetic algorithms, *Mechanical Systems and Signal Processing*, 12, 91-120.

Marwala, T. (2010), *Finite element model updating using computional intelligence techniques*, Springer-Verlag, London.

Möller, P.W., & Friberg, O. (1998), Updating large finite element models in structural dynamics, *AIAA Journal*, 36, 1861-1868.

Mottershead, J.E., & Foster, C.D. (1991), On the treatment of ill-conditioning in spatial parameter estimation from measured vibration data, *Mechanical Systems and Signal Processing*, 5, 139-154.

Mottershead, J.E., & Friswell, M.I. (1993), Model updating in structural dynamics: a survey, *Journal of Sound and Vibration*, 167, 347-375.

Nazmy, A.S., & Abdel-Ghaffar, A.M. (1990), Three-dimensional nonlinear static analysis of cable-stayed bridges, *Computers and Structures*, 34, 257-271.

Overschee, P.V., & Moor, B. (1996), *Subspace identification for the linear systems : theory–implementation*, Kluwer Academic Publishers, Netherlands.

Pedersen, M.E.H., & Chipperfield, A.J. (2010), Simplifying particle swarm optimization, *Applied Soft Computing Journal*, 10, 618-628.

Perera, R., & Torres, R. (2006), Structural damage detection via modal data with genetic algorithms, *Journal of Structural Engineering, ASCE*, 132, 1491-1501.

Perera, R., & Ruiz, A. (2008), A multistage FE updating procedure for damage identification in large-scale structures based on multiobjective evolutionary optimization, *Mechanical Systems and Signal Processing*, 22, 970-991.

Perera, R., Fang, S.-E., & Huerta, C. (2009a), Structural crack detection without updated baseline model by single and multiobjective optimization, *Mechanical Systems and Signal Processing*, 23, 752-768.

Perera, R., Ruiz, A., & Manzano, C. (2009b), Performance assessment of multicriteria damage identification genetic algorithms, *Computers and Structures*, 87, 120-127.

Perera, R., Fang, S.E., & Ruiz, A. (2010), Application of particle swarm optimization and genetic algorithms to multiobjective damage identification inverse problems with modelling errors, *Meccanica*, 45, 723-734.

Pintér, J. (1996), *Global optimization in action : continuous and Lipschitz optimization-algorithms, implementations, and applications*, Kluwer Academic Publishers, Boston.

Price, K., Storn, R.M., & Lampinen, J.A. (2005), *Differential evolution : a practical approach to global optimization*, Springer-Verlag, New York.

Proakis, J.G., & Manolakis, D.G. (1996), *Digital signal processing : principles, algorithms, and applications*, Prentice-Hall, Upper Saddle River, NJ.

Raich, A.M., & Liszkai, T.R. (2007), Improving the performance of structural damage detection methods using advanced genetic algorithms, *Journal of Structural Engineering, ASCE*, 133, 449-461.

Ren, W.X., & Peng, X.L. (2005), Baseline finite element modeling of a large span cable-stayed bridge through field ambient vibration tests, *Computers and Structures*, 83, 536-550.

Saada, M.M., Arafa, M.H., & Nassef, A.O. (2008), Finite element model updating approach to damage identification in beams using particle swarm optimization, *34th Design Automation Conference, ASME*, 522-531.

SAP2000 (2009), Structural Analysis Program, Computers and Structures, CA.

Storn, R., & Price, K. (1997), Differential evolution - a simple and efficient heuristic for global optimization over continuous spaces, *Journal of Global Optimization*, 11, 341-359.

Teughels, A., De Roeck, G., & Suykens, J.A. (2003), Global optimization by coupled local minimizers and its application to FE model updating, *Computers & Structures*, 81, 2337-2351.

Tikhonov, A.N. (1963), Regularization of incorrectly posed problems, *Soviet Mathematics*, 4, 1624–1627.

Titurus, B., & Friswell, M.I. (2008), Regularization in model updating, *International Journal for Numerical Methods in Engineering*, 75, 440-478.

Trelea, I.C. (2003), The particle swarm optimization algorithm : convergence analysis and parameter selection, *Information Processing Letters*, 85, 317-325.

Tu, Z., & Lu, Y. (2008), FE model updating using artificial boundary conditions with genetic algorithms, *Computers and Structures*, 86, 714-727.

Van Overschee, P., & De Moor, B. (1994), N4SID : subspace algorithms for the identification of combined deterministic-stochastic systems, *Automatica*, 30, 75-93.

Zárate, B.A., & Caicedo, J.M. (2008), Finite element model updating : multiple alternatives, *Engineering Structures*, 30, 3724-3730.

Zheng, Y.L., Ma, L.H., Zhang, L.Y., & Qian, J.X. (2003), On the convergence analysis and parameter selection in particle swarm optimization, *International Conference on Machine Learning and Cybernetics*, 3, 1802-1807.

Zivanovic, S., Pavic, A., & Reynolds, P. (2007), Finite element modelling and updating of a lively footbridge : the complete process, *Journal of Sound and Vibration*, 301, 126-145.

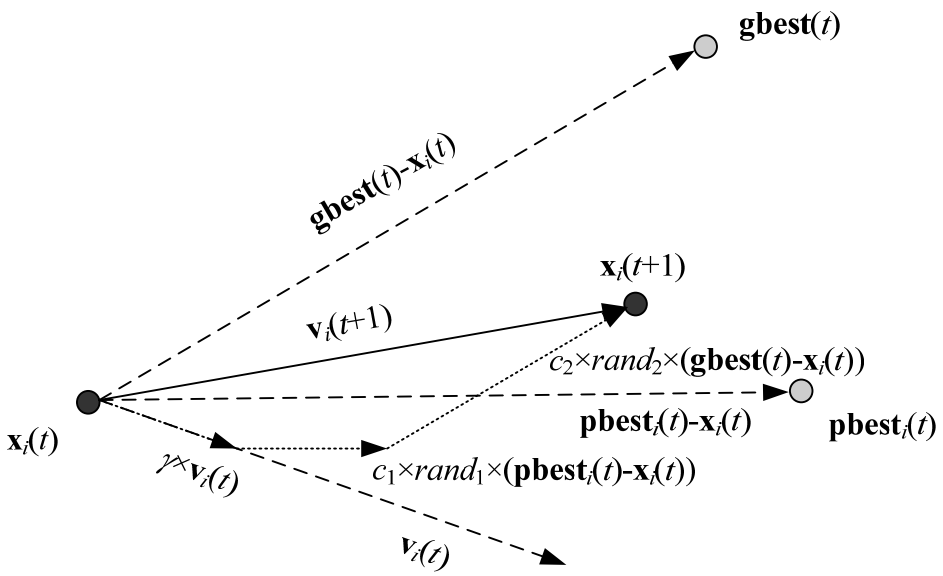

Figure 1. Pictorial view of particle behavior showing position and velocity update.

Figure 2. Full-scale cable-stayed footbridge.

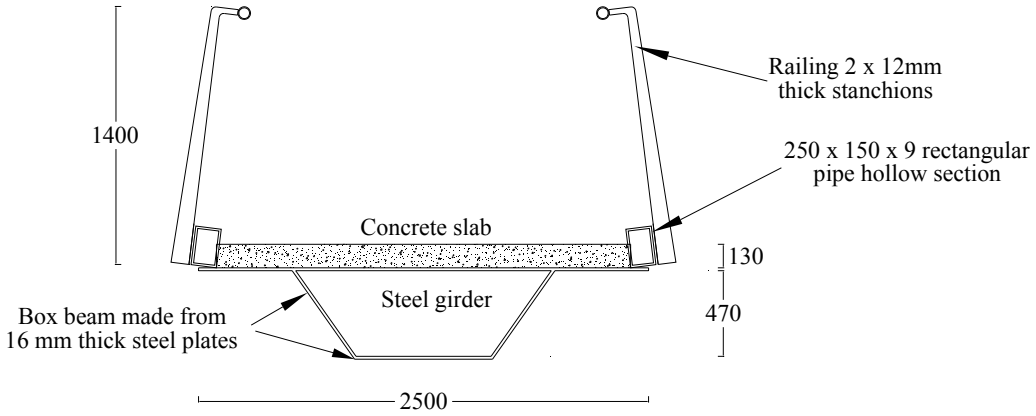

Figure 3. Cross-section of bridge deck (all dimensions in mm).

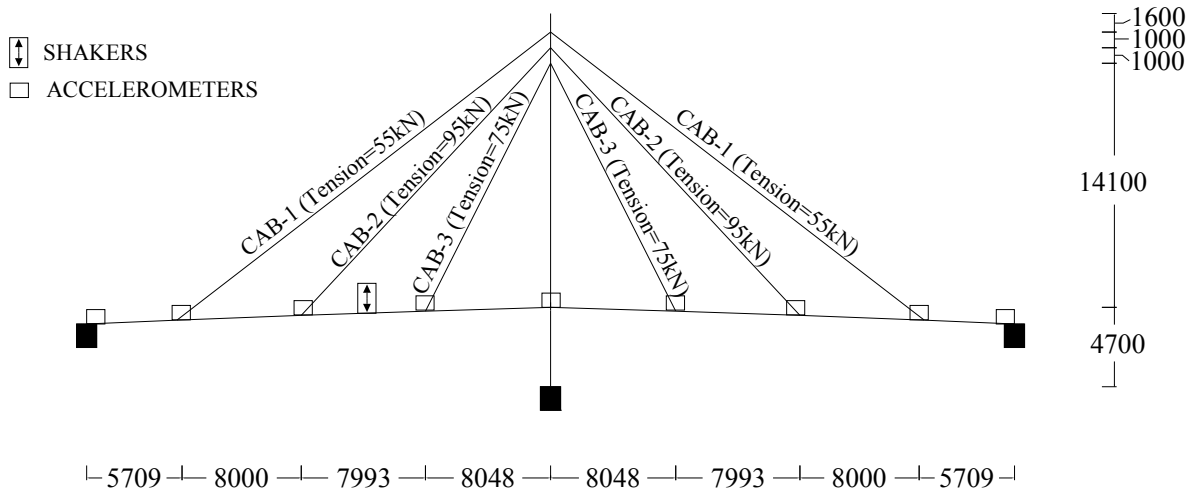

Figure 4. Basic bridge dimensions, cable post-tension forces and location of shakers and accelerometers in the experiment (all dimensions in mm).

Figure 5. Accelerometers (in the center) and shakers (at the back) placed on the bridge.

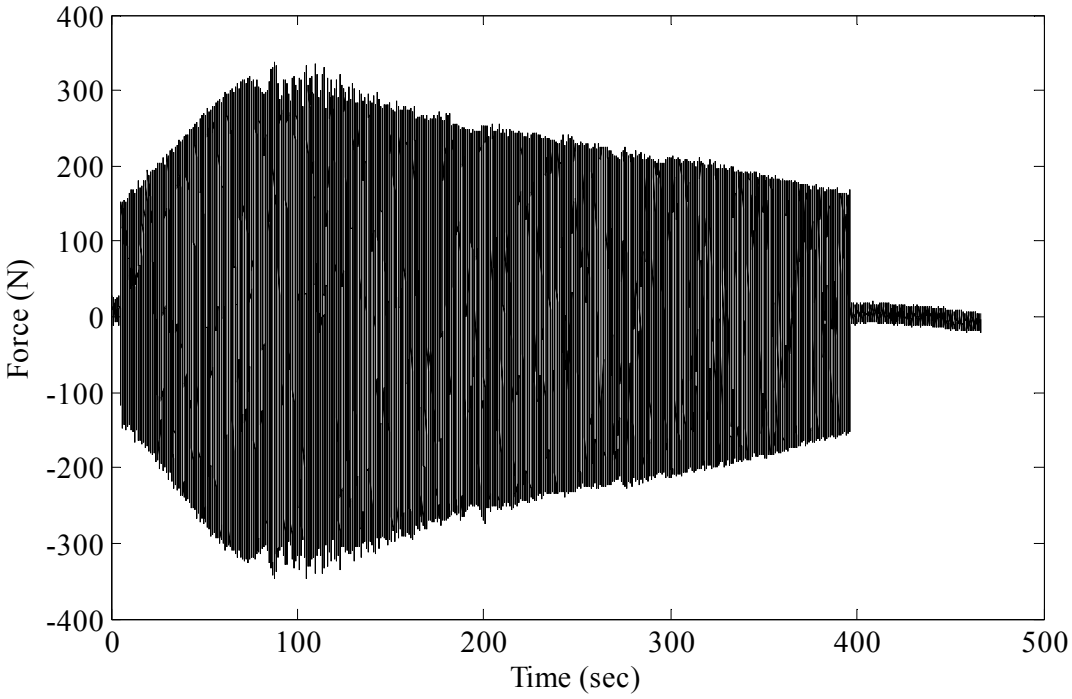

Figure 6. Time history of force applied by a shaker.

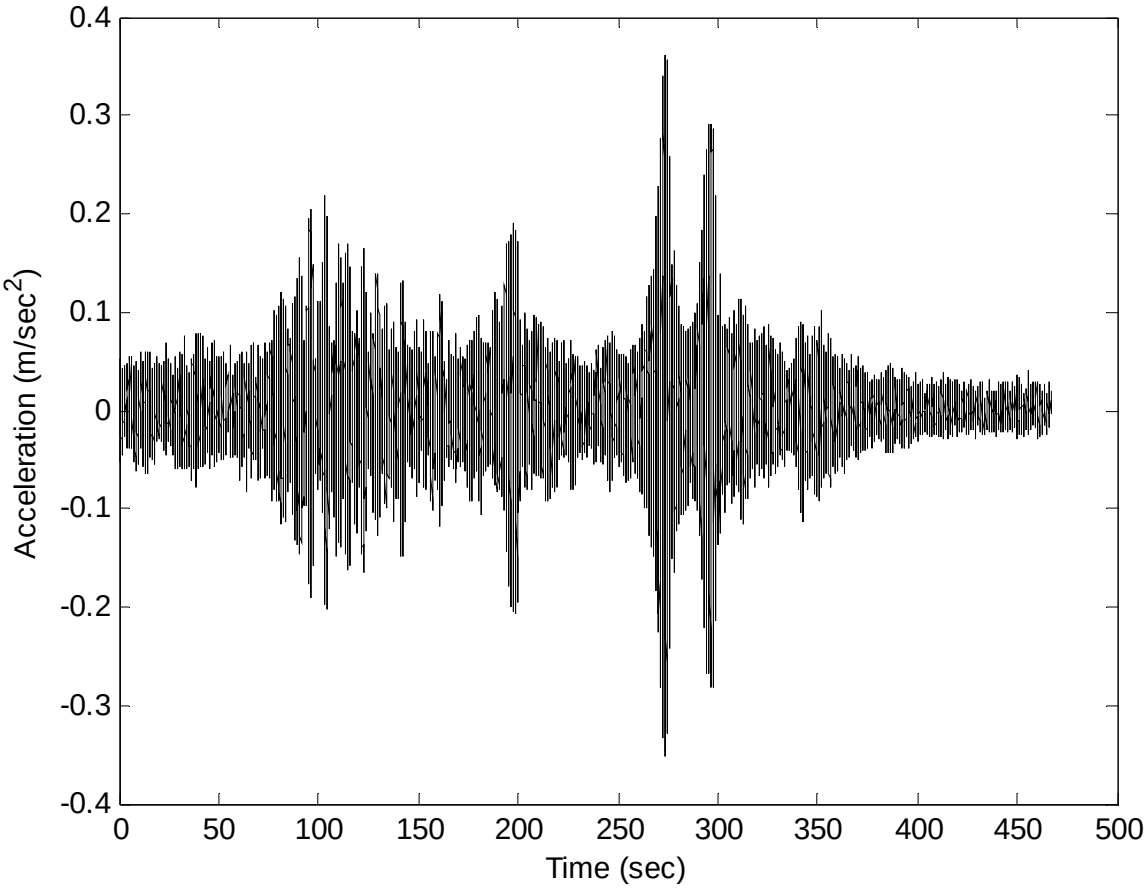

Figure 7. Time history of bridge response recorded during vertical shaker excitation.

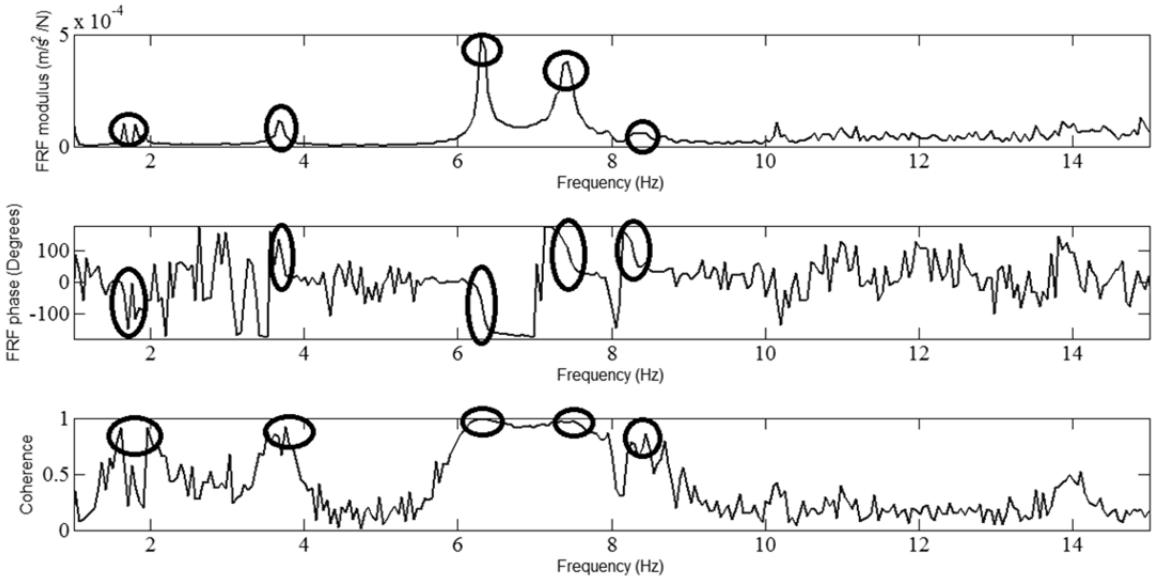

Figure 8. FRF measured during vertical shaker test.

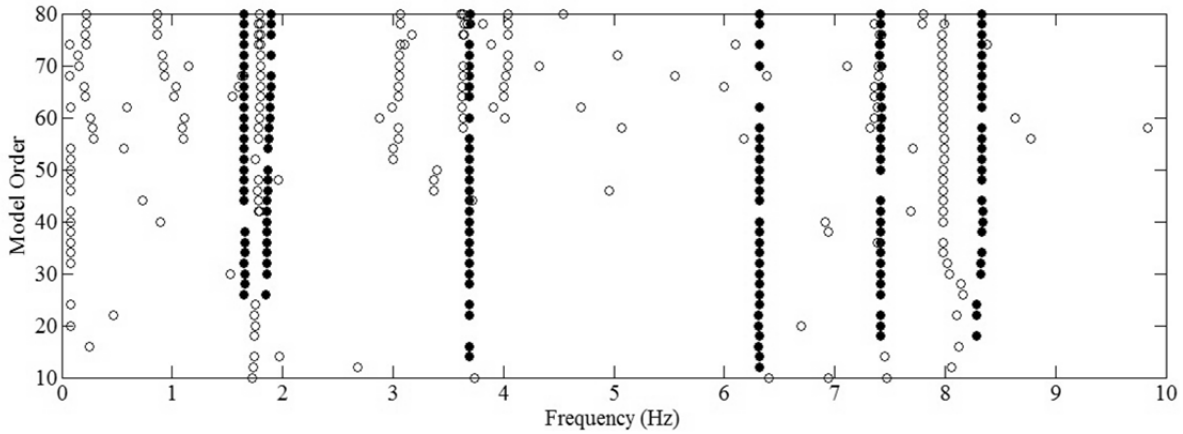

Figure 9. Stability diagram for a vertical shaker test (black dots indicate stable modes).

Mode 1 (1st vertical): Frequency 1.64 Hz

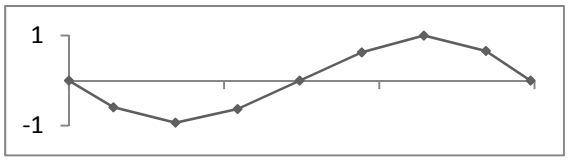

Mode 2 (2nd vertical): Frequency 1.89 Hz

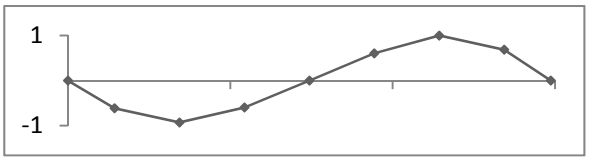

Mode 3 (3rd vertical): Frequency 3.69 Hz

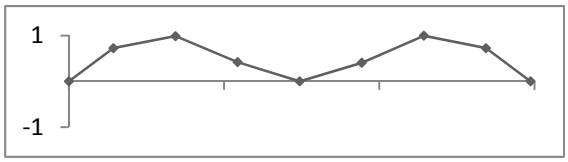

Mode 4 (1st horizontal): Frequency 4.86 Hz

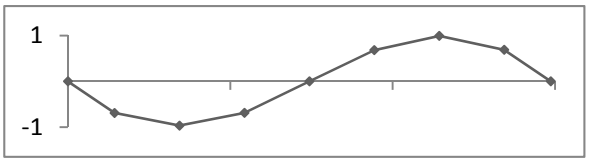

Mode 5 (1st horizontal): Frequency 5.33 Hz

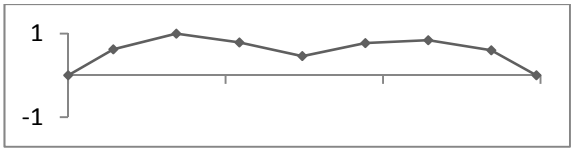

Mode 6 (4th vertical): Frequency 6.31 Hz

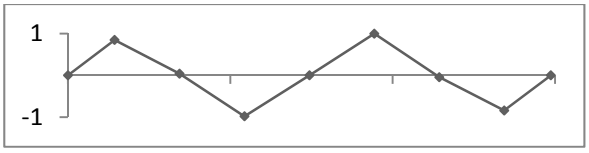

Mode 7 (5th vertical): Frequency 7.42 Hz

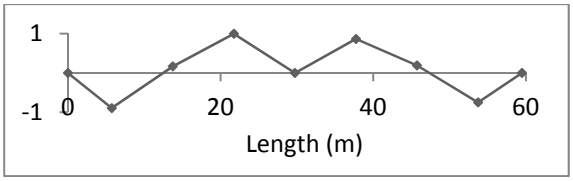

Mode 8 (1st torsional): Frequency 8.32 Hz

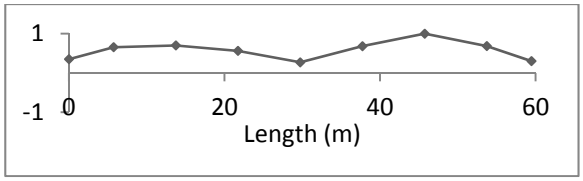

Figure 10. Normalized vertical, horizontal and torsional mode shapes identified using N4SID method.

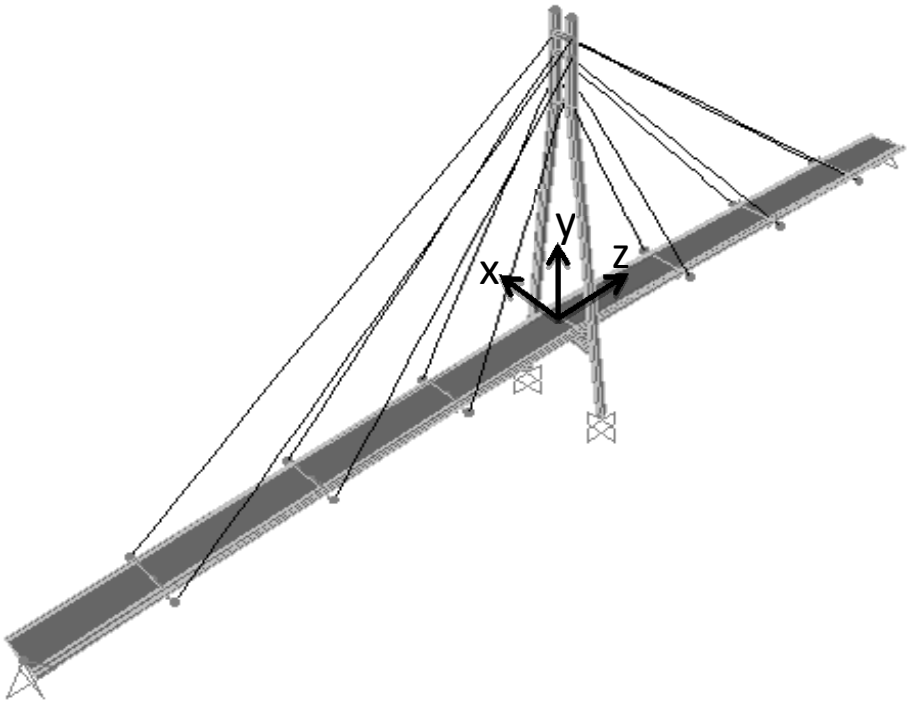

Figure 11. FE model of the bridge.

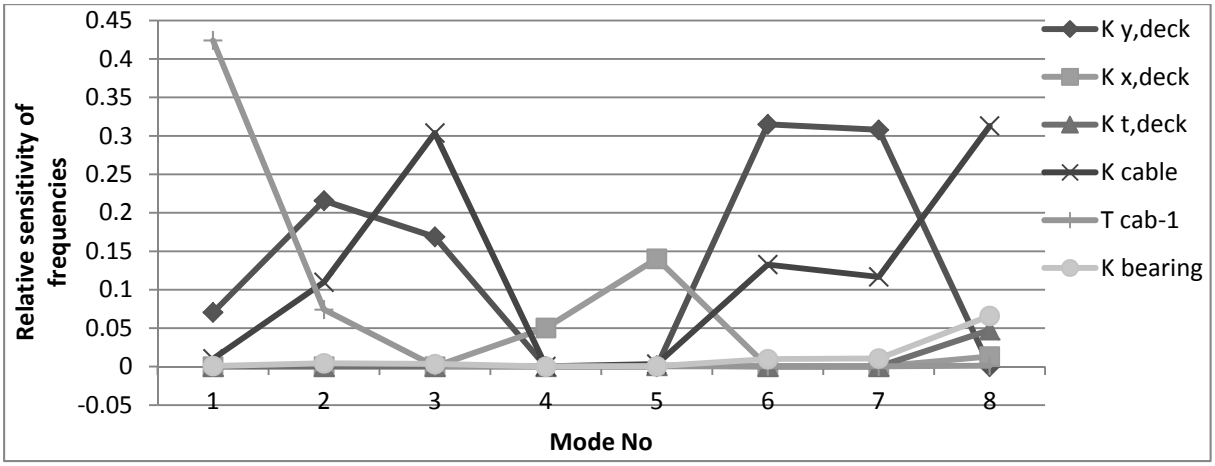

Figure 12. Sensitivity of modal frequencies to selected updating parameters.

Table 1. Experimentally identified natural frequencies and damping ratios.

Mode no.	Mode type	Experimental frequencies (Hz)		Damping ratios (%)
		Peak picking	N4SID	N4SID
1	1st vertical	1.64	1.64	0.2
2	2nd vertical	1.90	1.90	0.9
3	3rd vertical	3.66	3.69	0.5
4	1st horizontal	4.85	4.86	0.8
5	2nd horizontal	5.36	5.33	0.6
6	4th vertical	6.32	6.31	0.5
7	5th vertical	7.42	7.42	1.0
8	1st torsional	8.33	8.32	1.4

Table 2. Comparison between frequencies and mode shapes (MACs) between initial FE model and experiment.

Mode no.	Frequency			MAC
	Experiment by N4SID (Hz)	Initial FE model (Hz)	Error (%)	
1	1.64	1.66	1.22	0.999
2	1.90	1.88	-1.05	0.995
3	3.69	3.88	5.15	0.999
4	4.86	5.28	8.64	0.999
5	5.33	5.45	2.25	0.993
6	6.31	6.79	7.61	0.990
7	7.42	7.76	4.58	0.980
8	8.32	8.66	4.09	0.993

Table 3. Ratios of updated to initial stiffness and final objective function values for PSO alone.

Ratio of updated to initial stiffness (standard deviation)						Final value of objective function
$K_{y,deck}$	$K_{x,deck}$	$K_{t,deck}$	K_{cable}	$T_{Cab\text{-}1}$	$K_{bearing}$	
0.845 (0.0006)	0.837 (0.0003)	0.935 (0.0001)	0.925 (0.0020)	1.160 (0.0011)	0.932 (0.0058)	0.0021

Table 4. Ratios of updated to initial stiffness and final objective function values for PSO with SNT.

Minimum no.	Ratio of updated to initial stiffness						Final value of objective function
	$K_{y,deck}$	$K_{x,deck}$	$K_{t,deck}$	K_{cable}	$T_{Cab\text{-}1}$	$K_{bearing}$	
1	0.845	0.837	0.935	0.925	1.160	0.932	0.0021
2	0.662	0.798	0.600	1.300	1.044	0.600	0.0060
3	0.880	0.801	0.600	0.600	1.300	0.600	0.0049
4	0.600	0.802	0.957	1.300	1.219	0.950	0.0079

Table 5. Updated and experimental frequencies and MACs using PSO method.

Mode no.	Experimental frequencies by N4SID (Hz)	Updated FE model frequencies (Hz)	Error in frequencies (%)	MAC
1	1.64	1.69	2.84	0.999
2	1.90	1.86	-2.05	0.996
3	3.69	3.70	0.22	0.999
4	4.86	4.97	2.16	0.990
5	5.33	5.28	-1.03	0.987
6	6.31	6.39	1.23	1.000
7	7.42	7.30	-1.61	0.992
8	8.32	8.41	1.05	0.993